Received: 12 August 2024 | Revised: 26 September 2024 | Accepted: 12 October 2024 | Published online: 17 October 2024

RESEARCH ARTICLE

Archives of Advanced Engineering Science
2024, Vol. 00(00) 1–10
DOI: 10.47852/bonviewAAES42024076

BON VIEW PUBLISHING

Aging Retardation of Lead-Acid Batteries by Adjusting Charge Controller Threshold Values in Off-grid Photovoltaic System

Cihan Karaman[1,*]

[1]*Project Department, Cihan Karaman Sole Proprietorship Company, Türkiye*

Abstract: Hybrid systems or coupled power plants with energy storage are becoming more and more popular due to the rising need for energy. Researchers have been conducting several experiments to assure longer-lasting battery use due to the increasingly widespread use of energy storage and the depletion of resources such as silicon and precious metals. In this study, a simulation study is carried out in PVSyst software on lead-acid batteries, which have a low cycle and a very traditional electrochemical structure. The simulation is realized by scaling Spain's consumption curve in 2023, taken from the European Network of Transmission System Operators for Electricity, together with lead-acid batteries and off-grid photovoltaic modules. After the off-grid system design is created and consumption data are imported, it is aimed to extend battery life by changing the charge-discharge threshold values of the charge controllers. Threshold values are in two categories, high and low, and seventeen different cases are simulated. According to the results of the simulation, the state of charge levels of the batteries decrease significantly due to radiation and cloudiness in the winter months and remain high in the spring and summer months. When charge controllers are set to high threshold levels, they cause gassing currents that rise to an average of 20 amps, while battery life extends up to 5.3 years. When low threshold values are used, negligible levels of oxygen and hydrogen gasses are formed in the battery, but battery life decreases to 4.1 years.

Keywords: lead-acid battery, consumption, aging, simulation, threshold, photovoltaic system

1. Introduction

Since the industrial revolution, increases in carbon dioxide levels caused by the use of fossil resources have led to the creation of a number of action plans for the world [1]. The most important of these plans is the Paris Climate Agreement. According to this agreement, it is desired to keep the global air temperature increase below 1.5 °C, and thus, it is aimed to reduce greenhouse gas emissions [2]. In addition, various legal regulations aiming to bring battery technologies to the market at affordable costs, such as the Inflation Reduction Act in the United States, the Net Zero Industry Act in the European Union, and the production-linked incentive in India, have been put into effect [3]. The purpose of these action plans is to prevent climate change caused by greenhouse gases and leave a cleaner world for future generations [4]. According to a report using data from the World Meteorological Organization, the daily temperature rose to 50 °C and above between July 2023 and July 2024. The increase in air temperature leads to fires around the world, a decrease in the yield of agricultural products, disruption of energy, water, transportation, and communication facilities, and a decrease in the performance of students in education in non-air-conditioned environments [5]. For a cleaner world, the installation of wind and solar power plants, which are the most popular and clean energy sources of recent times, is increasing day by day [6]. However, integrating these systems into the grid requires that the grid infrastructure, energy continuity, and system reliability be strong and robust [7]. While a 220 GW power plant was installed in 2022 solar energy as a solution to the negative effects of climate change on human life, it is predicted that this figure will increase to 500 GW in 2030 [8].

In the electrical grid, production and consumption must always be in balance [9, 10]. Unfortunately, this becomes very difficult with sources that provide weather-dependent and intermittent energy production, such as solar and wind power plants [11]. In such cases, ups and downs can be observed in the system frequency or busbar voltage levels [12, 13]. For example, in an electrical network, there are a number of electrical loads that draw active and reactive current. And the current and power required by these loads at the desired time must be met by the generating plants. If the current consumption value is higher than the production value, then there will be a decrease in frequency, and we can only fix this issue, by increasing production. In this case, energy storage systems can meet this need in certain periods of time. So, the transition to energy storage systems coupled with that power plants is starting nowadays [14]. Battery systems, which are generally used as ancillary services such as inertial response, fast frequency response, primary frequency response, frequency regulation, ramping reserves, contingency spinning reserves, replacement non-spin reserves, voltage support, and black start capability, become a part of the continuous energy source in places where there is no energy. In addition, battery systems also

*Corresponding author: Cihan Karaman, Project Department, Cihan Karaman Sole Proprietorship Company, Türkiye. Email: proje@ckaraman.com.tr; cihan.karaman13@gmail.com

provide power quality, voltage support, loss reduction, reliability, and resiliency at transmission, distribution, and end-user points [15].

When using off-grid systems, the long-lasting and efficient use of batteries is of great importance for the user. Today's battery technology is evolving towards lithium-ion batteries with high energy density and long cycles [16]. In current battery technologies, lithium-nickel-cobalt-aluminum oxide, nickel-manganese-cobalt (NMC), and lithium-iron-phosphate batteries are mainly used. But since the cobalt is a very toxic and expensive element in NMC batteries, researchers are trying to design this battery without cobalt. By increasing the amount of nickel, it is aimed to provide high energy densities [17]. Lead-acid batteries with low energy density and cycles are slowly disappearing from the market. In addition to the developments in batteries, increasing battery usage poses a great threat in terms of resource depletion and non-recyclability [18]. As a solution to this problem, using batteries efficiently or in a healthy way can slow down the speed of this danger a little.

Generally, battery charge controllers adjust the charging and discharging thresholds of the battery without causing any damage to the electrolyte in the battery. However, in this study, charge and discharge thresholds are simulated at different values in order to extend the total cycling life of the battery. In this case, the electrolyte inside will deteriorate, but we will be able to use the battery for a longer time. What these threshold values will be is investigated.

In this study, an off-grid photovoltaic system with low-cycle lead-acid batteries is designed. Madrid, Spain, is selected for irradiation data. Annual hourly consumption data for Spain are obtained from the European Network of Transmission System Operators for Electricity transparency platform and scaled to create a small-size off-grid system. Production and consumption data are matched annually on an hourly basis on the PVSyst software, and battery aging times are calculated.

2. Literature Review

Battery technologies are in a wide range, and the main types include lithium-ion, lead-acid, sodium-sulfur, zinc-bromine, nickel-cadmium, vanadium-redox, and polysulfide bromine batteries [19]. Among them, lead-acid batteries stand out with their very cheap prices [20]. While the price for lead-acid batteries is between 189 and 297 euros per kWh of energy, including installation and transportation, this price is between 483 and 500 euros for lithium-ion batteries [21]. Just like lithium-ion batteries, lead-acid batteries can be connected to each other in series or parallel, depending on the desired power and voltage values. The lifespan of lead-acid and lithium-ion batteries decreases over time, and it is divided into two categories, which are calendar and cycling life [22, 23]. Calendar life refers to the life resulting from the battery's self-discharge when not in use [24], and cycling life refers to the life resulting from the completion of the battery's charging and discharging cycles.

Factors affecting battery life are the electrochemical properties of batteries, charge-discharge current rates, SOC, depth of discharge (DOD), and operating temperature [25, 26].

Lead-acid batteries consist of an electrolyte containing sulfuric acid and water and two positive and negative polarized electrodes containing lead and lead-oxide. During discharge, sulfate ions in the sulfuric acid surround the lead electrodes and enable electron flow, and in the meantime, the proportion of sulfuric acid in the electrolyte decreases [27]. During charging, sulfate ions release themselves back into the electrolyte, and this process occurs repeatedly in each charge-discharge phase [28]. As a result of the increase in operating temperature, the sulfate ions surrounding the electrodes crystallize and become a solid layer, and this situation is explained as sulfation in the literature [29]. As the operating temperature increases, the reaction rate in the electrolyte increases, but as a result of sulfation, internal resistance increases and battery voltage decreases. This is an indication that battery has reached the end of its life. Generally charging and discharging problems occur in batteries as a result of sulfation [30]. Sulfation builds up when the cutoff voltage reaches, preventing sufficient charge flow. Sulfation arises when the cell voltage surpasses the cutoff voltage prior to the accepted charge amount matching the discharge amount [31].

The situation takes on a different dimension when batteries operate in very cold weather. In batteries operating in cold weather, the electrolyte inside the battery freezes, and the battery again experiences charging and discharging problems [32]. Explanation of this situation is so. Since lead-acid batteries contain water along with sulfuric acid in the electrolyte, lead-acid batteries usually freeze at 0 °C ambient temperature. When freezing occurs, the solution inside the battery becomes solid, prevents the movement of ions, and does not allow electrochemical reactions to occur. The same situation occurs in lithium-ion batteries below 0 °C. Even batteries that can withstand ambient conditions of −40 °C lose 78% of their capacity [33]. According to a study, if batteries are used in high ambient temperatures, cell voltages decrease from 2.1 volts to 1.85 volts, and after 120 cycles, the discharge duration at 40 °C is 2 h, while at 0 °C the discharge duration is 3.8 h. After using the batteries for 50 cycles, the discharge capacity of the battery operated at 40 °C is 2 Ah, while the discharge capacity of the battery operated at −10 °C is 1 Ah. The reason for this is that as the temperature decreases, the internal resistance increases and the capacity decreases [34].

Another negative situation caused by high operating temperature is the formation of gassing currents. Production of hydrogen gas, which occurs when the battery is exposed to extreme temperatures, also occurs when the battery is overcharged more than 80% of SOC [35]. Again, according to a study conducted in the military, as the temperature increases, electrolyte resistance decreases and the mobility of ions increases, which causes the high-rate production of hydrogen gas in the battery [36]. In the study, gassing current is formulated with the derivation of Faraday's law as follows:

$$I_{gas} = \frac{R_v \times \frac{k}{100} \times \frac{273}{T+273} \times 1,608}{\frac{11,200}{28,316}} \quad (1)$$

where:

Igas: gassing current, T: temperature of ventilating air in °C, R_V: Rate of ventilation per minute [cubic feet of ventilating air], k: H_2% [percent of hydrogen].

Explanation of the formula: Based on the Faraday law, the formula indicates that an electrode will release one equivalent, or 1.008 grams, of hydrogen in 96,500 coulombs (ampere-seconds). At 0°C and 1 atmospheric pressure, this hydrogen will occupy a volume of 11,200 cubic centimeters (cc). Since the rate of ventilation is measured in cubic feet of ventilating air per minute, the 96,500 ampere-seconds must be converted to ampere-minutes with 1,608. The conversion factor from the cc to cu.ft. is 28,316 and number of 273 is used to convert Celsius to Kelvin [36].

Another study explained the effect of temperature on gassing current with the modified Tafel equation as follows [37]:

$$I_{gas} = b \times I_{G0} \times e^{g} \quad (2)$$

Figure 1
Circuit diagram of the off-grid system

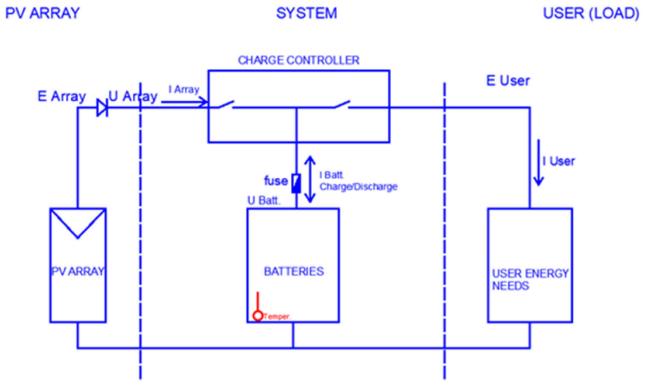

Figure 2
Flow chart of the simulation

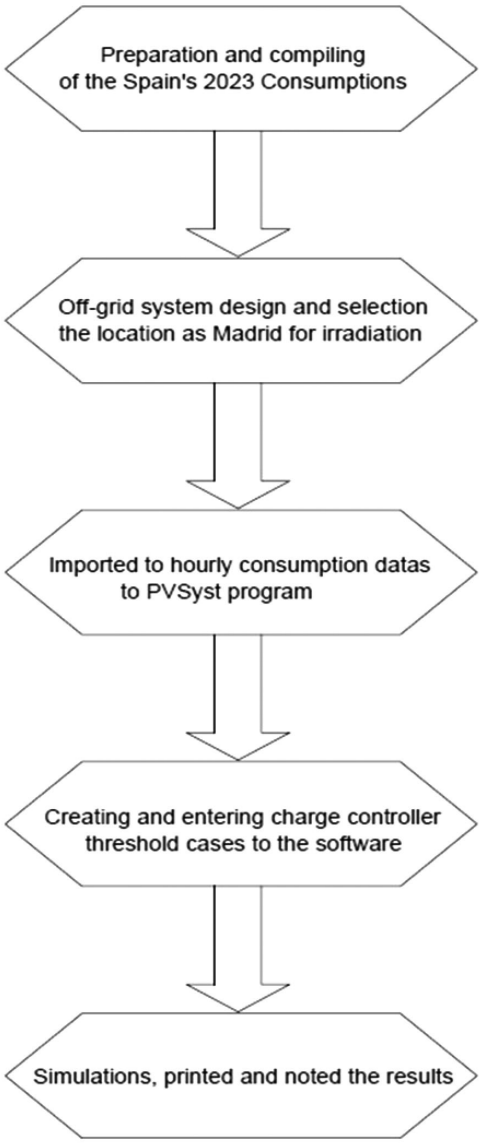

$$\mathfrak{b} = \frac{C_{10}}{100} \tag{3}$$

$$\mathfrak{g} = c_U \times (U - 2.23) + c_T \times (T_{batt} - 20) \tag{4}$$

where:

Igas: overall gassing current, I_{G0}: normalized gassing current [Ah], c_U and c_T: voltage $[V^{-1}]$ and temperature $[K^{-1}]$ coefficient, U: battery voltage per cells, T_{batt}: battery temperature, C_{10}: nominal capacity of the battery [Ah], Normalization conditions are 2.23 [V/cell] and 20 °C and a battery with a nominal capacity of 100 Ah.

Another issue that affects the aging of batteries is the high charge and discharge rates of batteries. It is called as C-rate of battery. Batteries operating at low charge and discharge rates draw less current and carry out their chemical reactions for a longer time. However, batteries operating with high C-rates react in a short time and complete their cycling life rapidly [38]. If this issue needs to be explained in more detail, each battery has a life cycle and the total amount of energy it stores. Depending on variable load requirements for a 100 amperes-hour battery, loads may sometimes draw 2 amperes of current or draw 50 amperes of current. If 2 amperes of current are drawn from the batteries, the duration for the battery to be fully discharged will be longer, and therefore it will complete its cycle in a long time. However, if 50 amperes of current are drawn, the battery will be discharged very quickly, which will cause the battery's life to run out quickly.

In a study, setpoints of SOC are determined to calculate the shortest charging times on lead-acid, lithium-ion, and nickel-metal hydride batteries. Here, two different setpoint adjustment methods are being investigated because long battery charging time has detrimental effects on the structure and properties of the battery. One of these methods was carried out by keeping the charging constant current (CC) and the other by keeping the charging constant voltage (CV). The batteries were charged with CC for a certain period of time and with the CV method for the remaining period, from 0%, 30%, and 50% charging initial rates until they were fully charged. The simulation was carried out on Matlab Simulink, and when the lead-acid battery was charged with CC while it was completely discharged and continued charging by applying CV at 55% of SOC, the total charging time was 14,056 h. If the setpoint value was set to 95%, the total charging time was 7,277 h. When the lead-acid battery is 30% charged and the setpoint value is set to 55%, the time required to fully charge is 12,528 h, while when the setpoint value is set to 95%, this time decreases to 5,682 h in total. When the battery is 50% charged and the setpoint values are adjusted to 55% and 95%, the total charging times are 11,531 and 4,619 h. Among the batteries, the one that charged in the shortest time was the lithium-ion battery with 2,632 h at 95% setpoint value [39].

Although using CC and CV charging methods together is a very mature method, it is not very suitable for fast charging. The CV stage causes the battery temperature to increase and the battery cycle to decrease, which also extends the charging time [40, 41]. Therefore, there is a transition to fuzzy logic control and predictive control models, and they are becoming widespread. In the fuzzy logic control model, batteries are charged with a very high current of up to 70% of SOC, and then, the current decreases exponentially by keeping the battery voltage constant. The predictive control model was used in a study for the purpose of frequency regulation of grid-connected systems. In this case, the batteries are set to work in two different scenarios. In the first scenario, setpoints are between 40% and 80%, while in the second case they are between 10% and 50%. In the first scenario,

maximum battery charge was reached in 17 min, while in the second case, this time increased to 80 min approximately [42].

In another implementing study, in a scenario where batteries stored energy with photovoltaic systems when energy prices were high and used when energy prices decreased, charge-discharge threshold values were used between 20% and 100% for the health of the batteries [43].

In an experimental study, it is stated that with an algorithm programmed using Arduino Uno R3 with a hybrid charging control unit that is charged both by solar panels and the grid, charging times are faster than traditional charging control mechanisms [44].

Another attractive and well-informed study describes disconnection and reconnection threshold tests on the charging states of batteries. In this study, five different charging threshold values were examined. While the charging disconnection voltages for cases A, B, C, D, and E were determined to be 14.6, 14.4, 13.8, 14.0, and 14.4 volts, the reconnection threshold values were 13.7, -, 13.5, 12.9, and 13.6 volts, respectively. When case A is tested, the SOC of the battery value reaches 96% due to the high disconnection voltage (14.6 V). At the same time, since the reconnection threshold value is high, too many reconnection and disconnection cycles will occur in a short time, which can damage the MOSFETs that perform switching functions. In case B, the PWM charge controller device was tested. In this case, SOC of the battery is at 95%, and since the PWM charge controller will continue to provide CV when the battery reaches the disconnection voltage, water loss and corrosion that may occur in the battery must be prevented. In case C, the battery disconnection threshold value was selected as low, and SOC of the battery value dropped to 80%. In addition, since the range of disconnection and reconnection threshold values is very narrow, very rapid cycles will occur within the battery itself, which will cause the internal resistance of the battery to remain high. In case of D, the battery disconnection threshold value is normal, but the reconnection setpoint is under the open circuit voltage of the battery. This means that during the daytime, when there is no load, the battery cannot reach the reconnection voltage, and, as a result, solar energy will be wasted. The study states that the maximum DOD of gel batteries should not go below 30% and that charge disconnection voltage range of the batteries with a 12 V system voltage should be between 13.8 and 14.4 volts. The reconnection voltage value range should be between 13.0 and 13.5 V for batteries with a 12 V system voltage [45].

3. Design of the Study

The study begins with the compilation of annual consumption data from the European Network of Transmission System Operators for Electricity. The location chosen is Madrid, Spain. Sunshine data are obtained from PVSyst for this location. However, the consumption curve consists of general dataset for the entire Spanish country realized in 2023, and since the data for the entire country is a very large system, this data has been scaled for a small capacity system. Figure 1 shows the basic circuit diagram of the off-grid system, and Figure 2 shows the flow chart of the simulation. Figure 3 below shows the annual consumption curve on an hourly basis. According to this dataset, while electricity consumption reaches peak levels in winter and summer, this amount decreases slightly in spring.

The average consumption value is 1.308 kW per hour, resulting in a total annual consumption of 11,465.58 kWh.

Solar energy values are taken from the Meteonorm 8.1 in PVSyst 7.4, and the annual global irradiation chart on a daily basis is shown in Figure 4. Figure 5 shows the monthly global irradiation for Madrid, Spain. According to these values, maximum total monthly irradiation is 243.3 kWh per square meter per month in July, and the minimum total irradiation is 58.2 kWh per square meter per month in December. Average air temperature is recorded as 15.8 °C in a year. In addition, since the air temperature is not so high in Spain, the voltages of the solar panels remain at high levels, and more power is obtained. In the study, 24 units of solar panels of the Seraphim brand with a power of 450 watts, 6 units of mppt converters of the Leonics brand with a power of 1,600 watts, and 40 units of Deka brand sealed lead-acid gel batteries with a voltage level of 12 Volts are used. Information about components is shown, respectively, in

Figure 3
Yearly scaled consumption data for 2023

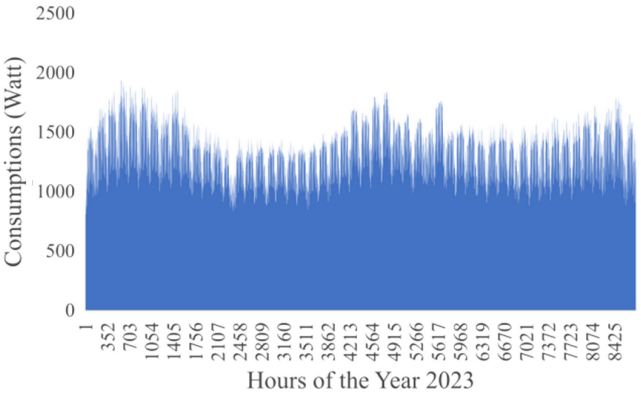

Figure 4
Yearly global horizontal irradiation for Madrid

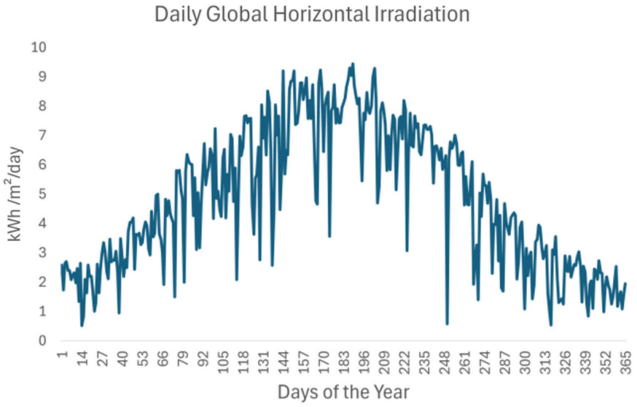

Figure 5
Global horizontal irradiation for Madrid, Spain

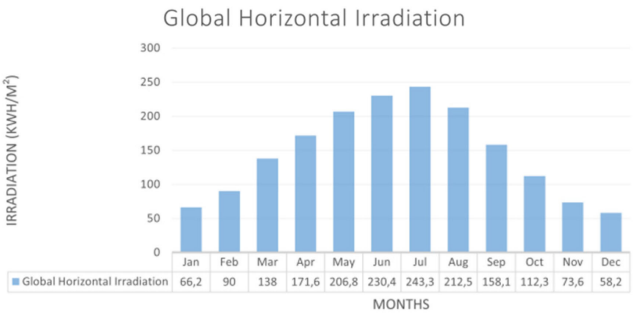

Table 1
Seraphim 450 watts solar panel information

Specifications	Values	Units
Short circuit current (Isc)	11.41	Amper
Maximum current (Impp)	10.77	Amper
Open circuit voltage (Voc)	50.10	Volt
Maximum voltage (Vmpp)	41.80	Volt

Table 2
Leonics SPT 4830 mppt converter information

Specifications	Values	Units
Max. charging current	20	Amper
Max. discharging current	10	Amper
Converter nominal power	1,600	Watts
Self-consumption	35	milliampere
Night consumption	35	milliampere

Table 3
Deka lead-acid gel battery information

Specifications	Values	Units
Nb of elements in series	6	unit
Nominal voltage	12	Volt
Capacity at C10	169	Ah
Internal resistance	14.2	milliohm
Coulombic efficiency	97	%

Tables 1, 2, and 3 below.Global horizontal irradiation for Madrid, Spain

The total DC panel power is 10.8 kWp, and the total battery system voltage is 48 volts. This voltage is obtained by connecting four batteries with a 12-volt series. The life of the batteries is 224 cycles. The total stored energy during the battery life is 15,583 kWh. Loss of load probability and autonomy periods are 2% and 2 days, respectively, in the simulation. Total AC MPPT converter power is 9.60 kW. There is no use of a generator as a backup power supply.

As can be seen from Figure 6 below which is embedded graph in PVSyst, there is a positive relationship between gassing and overcharging. The axis on the left shows the current fraction that causes the battery to gas during charging. The lower axis shows the SOC of the battery. When the battery starts to be charged above 85%, gassing current begins to show itself on the battery. When charged above 90%, 20% of the charging current causes gassing. This situation increases exponentially, and in a battery charged to 96%, 60% of the charging current causes gassing.

Continuing from where sulfation was explained above, even if the batteries do not reach the cutoff voltage, if the cell voltage is sufficiently greater than the open circuit voltage of fully charged battery, electrolyte dissociation occurs in the water and hydrogen and oxygen gases are released. This is a broader explanation of gassing in the batteries [31]. In a study, lithium-iron-phosphate batteries are overcharged at different C-rates, and it is seen that as charging rates increase, electrolyte degradation accelerates, which increases the risk of explosion as a result of gassing in the batteries. In the study, the amount of hydrogen gas is 61%, 53%, and 50% for 2C, 1.5C, and 1C rates, respectively [46]. In another study conducted with lithium batteries, the effects of high current overcharge and discharge on battery aging are investigated, and sudden temperature increases occur in the batteries during charging with 4C rates, and the battery temperature value increases up to 140 °C during discharge [47].

In Figure 7 above which is embedded graph in PVSyst, the relationship between the DOD and the battery cycle is explained. At 10% of battery discharge, battery cycle is 3,500, while when half of the battery is discharged, the cycle drops to 600. After 80% of discharge, the battery cycle reaches its lowest levels.

There are a number of parameters that the PVSyst program uses as a basis when calculating battery voltage. First of all, the PVSyst software uses load flow data in hourly production and consumption to determine the SOC of the battery in the off-grid system. In addition, the operating temperature values of the battery can be entered into the program, and a battery voltage calculation is made according to these values. By keeping the internal resistance of the battery constant and considering that battery current is variable, the battery voltage can be simulated clearly by the software. It calculates the battery voltage according to battery's SOC, open circuit voltage, battery temperature and the battery's charging or discharging current and the formulation for calculating battery voltage is shown in the equation below.

$$U_{batt} = U_{oc} + (\alpha \times SOC) + \rho \times (T_{batt} - T_{ref}) + (R_i \times I_{batt}) \quad (5)$$

where:

Figure 6
Battery gassing-SOC relation

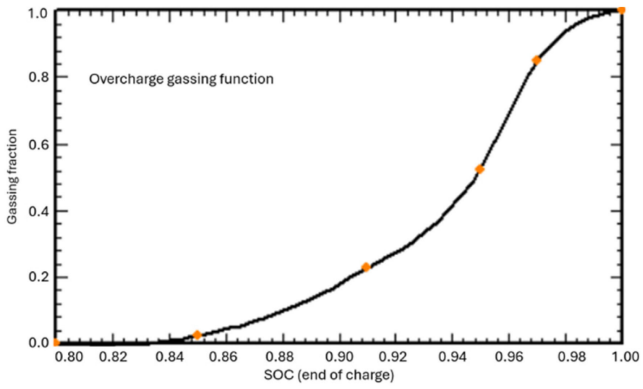

Figure 7
Battery cycle-SOC relation

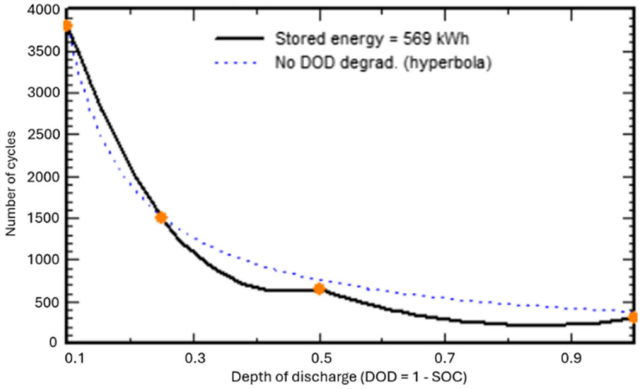

Table 4
Threshold cases of charge controller

Cases	Mode	Disc.	Rec.	Mode	Disc.	Rec.
Case-1	Cha.	0.83	0.60	Disch.	0.19	0.31
Case-2	Cha.	0.83	0.60	Disch.	0.27	0.42
Case-3	Cha.	0.83	0.60	Disch.	0.37	0.51
Case-4	Cha.	0.86	0.60	Disch.	0.19	0.35
Case-5	Cha.	0.83	0.60	Disch.	0.18	0.80
Case-6	Cha.	0.83	0.60	Disch.	0.51	0.65
Case-7	Cha.	0.90	0.60	Disch.	0.19	0.31
Case-8	Cha.	0.92	0.60	Disch.	0.19	0.35
Case-9	Cha.	0.90	0.75	Disch.	0.19	0.31
Case-10	Cha.	0.90	0.75	Disch.	0.19	0.45
Case-11	Cha.	0.99	0.85	Disch.	0.19	0.35
Case-12	Cha.	0.99	0.85	Disch.	0.19	0.60
Case-13	Cha.	0.99	0.85	Disch.	0.19	0.80
Case-14	Cha.	0.99	0.85	Disch.	0.37	0.51
Case-15	Cha.	0.99	0.85	Disch.	0.42	0.80
Case-16	Cha.	0.99	0.85	Disch.	0.57	0.80
Case-17	Cha.	0.99	0.60	Disch.	0.54	0.80

*Cha.: Charging, Disch.: Discharging, Disc.: Disconnection, Rec.: Reconnection

U_{batt}: battery voltage [V], U_{oc}: open circuit voltage [V], α: slope of the open circuit line (depends on the chemical couple Pb-SO4) SOC: state of charge, ρ: temperature coefficient (−5 to −6 mV/°C), T_{batt}: battery temperature, T_{ref}: reference temperature (20°C), R_i: internal resistance, assumed to be constant, I_{batt}: battery current (charge > 0, discharge < 0).

Explanation of the formula: Battery voltage shows the battery voltage calculated by the software; open circuit voltage is the voltage level measured from the poles of the battery when it is not connected to any load; for the slope of the open circuit line, the open circuit voltage is supposed to be linear as a function of SOC. The midpoint (SOC = 50%) is set to 2.045 V at 20 °C and the slope is 178.2 mV for the full SOC range; SOC is the state of charge of the battery; temperature coefficient shows the change in voltage according to the temperature value; internal resistance shows the resistance value of the battery to electrochemical reactions; battery current is the current value of the loads that draw from the battery; temperatures are related to the battery with a reference temperature value of 20 °C and the temperature entered to the program.

In this study, after generating production and consumption data with the battery, converter, and off-grid system, it is planned to extend the life of the batteries by changing the charge and discharge thresholds of the charge controller. For this purpose, 17 different threshold values are determined. While determining these values, calculations are made considering the charge and discharge limits of the PVSyst software. According to these limits, charging disconnection and reconnection values should be between 0.80–0.99 and 0.60–0.85 of SOC, while discharging disconnection and reconnection values should be between 0.10–0.60 and 0.25–0.80 of SOC. Accordingly, threshold cases are shown in Table 4 below.

4. Results of the Study

In this study, threshold values are divided into two parts. In the first application, the operation of the batteries is ensured by keeping the charge and discharge thresholds low, and in the second application, the system is operated by keeping these threshold values high. In the 0.83–0.60 SOC for charging and 0.19–0.31 SOC for discharging cases, the percentage of energy used directly from solar energy is 27.9%, while the percentage of energy used from the battery is 72.1%. In this case, the total charging time is 2,141.88 h, while the total discharge time is 6,512.41 h. Annual average battery voltage is 49.78 volts. The average charge and discharge currents are 73.40 and 24.43 amperes, respectively. While the average gassing current for this situation is 0.30 amperes, the total charge and discharge energy are 8,454.05 kWh and 8,043.60 kWh, respectively. When we examine this situation, we see that the battery is not overcharged and discharged. This keeps the gassing current value in the battery very low and calculates the battery life at 4.1 years. It meets 98% of the need for an annual load of 11,466 kWh, and only 179 kWh of missing energy occurs. 37% of energy is never used in the batteries for this case. The SOC graph of the battery for this situation is shown in Figure 8 below.

Figure 8
SOC of the Case-1

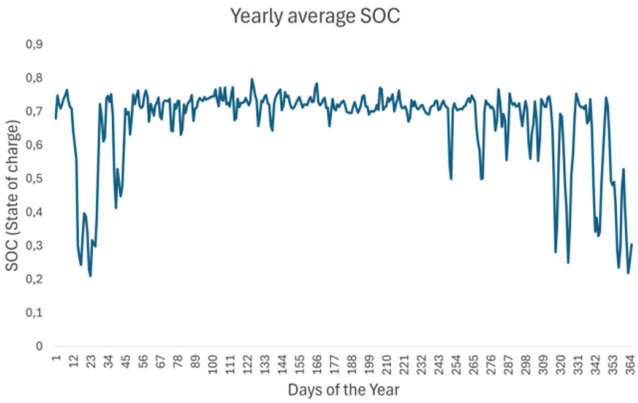

The SOC chart shows us that the charge level of the batteries drops to 20% during winter months. In summer and spring, batteries are at an average of 70% SOC.

Compared to the first case, when we keep the charging threshold value constant and increase the discharge threshold values to 0.51–0.65 SOC, the total charging time increases by 2 h and the discharge time decreases by 159 h. The average SOC value of the battery increases by 4%. While the average battery voltage increases at negligible levels, the gassing current value remains constant at 0.30 amperes. While total charging energy decreases by 1.58%, battery efficiency decreases by 0.5%. While the battery efficiency decreases slightly and the gassing current value remains constant, the life of the battery increases by 4.8 months, reaching a total of 4.5 years. In this case, the missing energy that can't reach the load side increases by 170% and becomes 482.04 kWh.

When we look at the results for this case, the battery life has increased, but amount of energy missing from the load has also increased. Since the first rule is that the energy coming to the load should not decrease, it is not so appropriate to increase the discharge threshold values while charging thresholds remain stable.

Figure 9 below shows the SOC curve of the battery for Case 6.

When we examine the SOC graph for Case 6, we cannot observe the extreme discharge situations that occur during the winter months on this curve. While the lowest SOC value is 0.5 in this graph, the average SOC value of the battery is 0.70 yearly.

Figure 10 below SOC curve belongs to Case 11. In this case, the battery charging threshold values have been increased to 0.99–0.85,

Figure 9
SOC of the Case-6

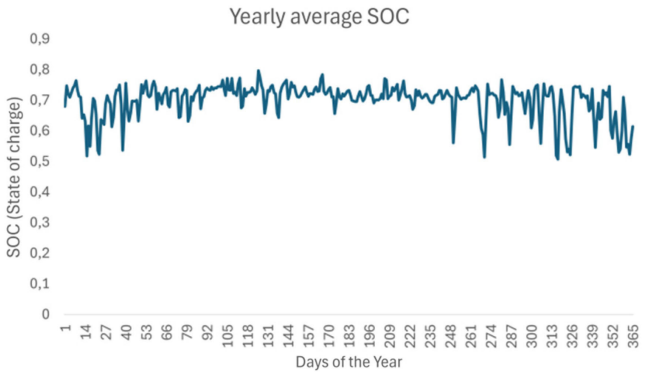

Figure 10
SOC of the Case-11

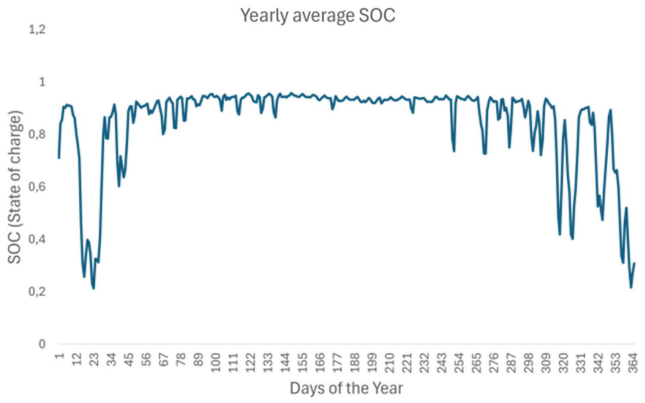

and the discharging threshold value has been adjusted to 0.19–0.35 SOC. When looking at the SOC graph for Case 11, batteries again tend to over-discharge during the winter months. However, on an annual basis, the average SOC value of the battery increases to 0.85.

While the total charging time increases to 3,291 h, the discharge time decreases to 5,420.80 h. The annual average battery voltage increases to 52.36 volts, and the average charging and discharging currents decrease negligibly. Gassing currents increase significantly and reach 20.11 amperes on average. While the efficiency of the battery decreases to 47.5%, the total charged energy increases to 13,532.62 kWh. The battery life has increased to 4.9 years. Tables 5 and 6 below show the battery life, charge and discharge energy, average battery voltages and gassing currents, charging and discharging hours for all cases.

If we compare the results of the study with previous ones, the determination of the discharging current of the battery is determined not by CC or voltage but by user needs. In the study carried out with the Arduino Uno R3 [44], it shortens the battery charging time, charges the batteries with a 12-volt system voltage when it drops below 10.8 volts, and cuts off the charging when it rises above 13.5 volts. In our study, solar panels charge batteries when the voltage drops below 12.52 volts and stop charging when the voltage rises above 13.55 volts. In this case, the battery aging time is 4.6 years, and the total battery charging time is 2,150.54 h. If we compare the results of the study examining charge control

Table 5
Results for all cases

	Aging	Ch.En.	Dis.En.	Voltage	Gas.
Case-1	4.1	8,454	8,043	49.7	0.30
Case-2	4.2	8,438	8,016	49.8	0.30
Case-3	4.3	8,397	7,968	49.8	0.30
Case-4	4.3	8,489	8,069	49.8	0.34
Case-5	4.3	8,426	7,977	49.8	0.30
Case-6	4.5	8,320	7,867	49.9	0.30
Case-7	4.5	8,539	8,059	50.1	0.58
Case-8	4.5	8,594	8,069	50.2	0.78
Case-9	4.6	8,539	8,059	50.1	0.58
Case-10	4.6	8,553	8,070	50.1	0.58
Case-11	4.9	13,532	6,440	52.3	20.1
Case-12	5.0	13,543	6,428	52.3	20.1
Case-13	5.0	13,560	6,413	52.3	20.1
Case-14	5.1	13,541	6,383	52.4	20.0
Case-15	5.2	13,575	6,322	52.5	19.9
Case-16	5.3	13,596	6,257	52.5	19.7
Case-17	5.3	13,590	6,287	52.5	19.7

*Aging: lifetime [years], Ch.En: charging energy [kWh], Dis.En: discharging energy [kWh], Gas.: gassing current [Amper]

Table 6
Results for all cases-2

	Average SOC	Charging hours	Discharging hours
Case-1	0.66	2,141.88	6,512.41
Case-2	0.67	2,147.79	6,488.72
Case-3	0.68	2,151.80	6,444.81
Case-4	0.68	2,140.51	6,529.96
Case-5	0.68	2,118.12	6,462.81
Case-6	0.70	2,143.03	6,353.14
Case-7	0.73	2,158.05	6,525.85
Case-8	0.74	2,163.93	6,532.83
Case-9	0.73	2,158.07	6,525.84
Case-10	0.73	2,150.54	6,536.97
Case-11	0.85	3,291.00	5,420.80
Case-12	0.85	3,292.00	5,415.66
Case-13	0.85	3,292.42	5,401.96
Case-14	0.86	3,293.00	5,374.30
Case-15	0.87	3,292.00	5,328.98
Case-16	0.89	3,322.00	5,267.91
Case-17	0.88	3,319.40	5,292.65

devices for five different cases [45], according to the high charge-discharge threshold values of the batteries, the DOD values of the gel batteries should not fall below 30%, the charge disconnection voltage values should be between 13.8 and 14.4 volts, and the charge reconnection values recommended should be between 13.0 and 13.5 volts. The DOD percentage values that match our study are for the cases of 14, 15, 16, and 17. In these cases, the overcharging method is applied, and the reconnection values were slightly below the recommended values.

5. Conclusion

When we look at the general results of the simulation, battery efficiency is quite high when we set the charge and discharge thresholds at low levels. When these thresholds are set high, battery

efficiency decreases significantly. Since batteries are used more at low charge-discharge thresholds, average SOC values are low compared to high threshold values. At high charge-discharging thresholds, serious gassing currents occur. At low threshold values, gassing currents are negligible. At low threshold values, batteries charge in a shorter time, while at high threshold values, they charge for a longer time. Discharge times for both threshold values are the opposite of charging times. When we use batteries at low thresholds, around 37% of the energy in the battery is not consumed at all. However, in batteries used at high thresholds, there is no unused energy. The most striking of the results is that while the lifespan of batteries used at high thresholds extends up to 5.3 years, the lifespan of batteries used at low charge-discharge thresholds starts at 4.1 years.

We know that currently used batteries primarily are protected by charge controllers as their working principle. However, in this study, we see that the lifespan of batteries becomes longer at different charge controller threshold values. The life of the battery increases from 4.1 years to 5.3 years. However, due to overcharging of the battery resulting in electrolyte dissociation, we see that significant amounts of hydrogen and oxygen gases are released in the battery. This may cause the battery to explode and cause a fire. It is important that this study sets an example for future studies. Batteries are generally like a sealed box. However, batteries need to be transformed into a machine with a cycle inside rather than a closed box. The gases that emerge when batteries operate at high charge and discharge thresholds must be expelled from the batteries through pressurized tubes, and the reduced electrolyte level must be increased again to eliminate the risk of battery explosion.

Of course, a debate arises here as to whether we should operate the battery at higher efficiency and replace it in a short time without damaging the electrolyte inside the batteries, or whether we should operate them at low efficiency and benefit from them for a longer time. My opinion on this subject is that when we consider depleted precious metals and energy sources, we need to operate a battery that will replace in the end at low efficiency, and if we are able to get energy from it, we need to operate the charge controllers at high charge-discharge thresholds.

Ethical Statement

This study does not contain any studies with human or animal subjects performed by the author.

Conflicts of Interest

The author declares that he has no conflicts of interest to this work.

Data Availability Statement

Data available on request from the corresponding author upon reasonable request.

Author Contribution Statement

Cihan Karaman: Conceptualization, Methodology, Software, Validation, Formal analysis, Investigation, Resources, Data curation, Writing – original draft, Writing – review & editing, Visualization, Supervision, project administration.

References

[1] Soylu, O. B., Turel, M., Balsalobre-Lorente, D., & Radulescu, M. (2024). Evaluating the impacts of renewable energy action plans: A synthetic control approach to the Turkish case. *Heliyon*, *10*(4), 1–14. https://doi.org/10.1016/j.heliyon.2024.e25902

[2] UNFCCC. (2015). ADOPTION OF THE PARIS AGREEMENT – Paris agreement text English.

[3] I. Energy Agency. (2024). World energy outlook special report batteries and secure energy transitions. [Online]. Retrieved from: www.iea.org

[4] Jain, P. C. (1993). Greenhouse effect and climate change: Scientific basis and overview. *Renewable Energy*, *3*(4), 403–420. https://doi.org/10.1016/0960-1481(93)90108-S

[5] United Nations Secretary-General's Call to Action on Extreme Heat. (2024). [Online]. Retrieved from: https://www.lancetcountdown.org/about-us/interact-with-the-key-findings/

[6] Hassan, Q., Algburi, S., Sameen, A. Z., Salman, H. M., & Jaszczur, M. (2023). A review of hybrid renewable energy systems: Solar and wind-powered solutions: Challenges, opportunities, and policy implications. Results in Engineering, *20*, 101621. https://doi.org/10.1016/j.rineng.2023.101621

[7] Khan, K. A., Quamar, M. M., Al-Qahtani, F. H., Asif, M., Alqahtani, M., & Khalid, M. (2023). Smart grid infrastructure and renewable energy deployment: A conceptual review of Saudi Arabia. *Energy Strategy Reviews*, *50*, 101247. https://doi.org/10.1016/j.esr.2023.101247

[8] I. – International Energy Agency, "World Energy Outlook 2023," (2023). [Online]. Retrieved from: www.iea.org/terms

[9] Barone, G., Buonomano, A., Forzano, C., Palombo, A., & Russo, G. (2023). The role of energy communities in electricity grid balancing: A flexible tool for smart grid power distribution optimization. *Renewable and Sustainable Energy Reviews*, *187*, 113742. https://doi.org/10.1016/j.rser.2023.113742

[10] Lezhniuk, P., Kozachuk, O., Komenda, N., & Malogulko, J. (2023). Electrical power and energy balance in the local electrical system by using reconciliation of the generation and consumption schedules. *Przeglad Elektrotechniczny*, *2023*(9), 57–63. https://doi.org/10.15199/48.2023.09.10

[11] Osman, A. I., Chen, L., Yang, M., Msigwa, G., Farghali, M., Fawzy, S., …, & Yap, P. S. (2023). Cost, environmental impact, and resilience of renewable energy under a changing climate: A review. *Environmental Chemistry Letters*, *21*(2), 741–764. https://doi.org/10.1007/s10311-022-01532-8

[12] Saha, S., Saleem, M. I., & Roy, T. K. (2023). Impact of high penetration of renewable energy sources on grid frequency behaviour. *International Journal of Electrical Power & Energy Systems*, *145*, 108701. https://doi.org/10.1016/j.ijepes.2022.108701

[13] Singh, M., & Singh, L. (2024). A comprehensive study of power quality improvement techniques in smart grids with renewable energy systems. In *Lecture Notes in Electrical Engineering, Springer Science and Business Media Deutschland GmbH*, 241–251. https://doi.org/10.1007/978-981-99-8289-9_18

[14] León Gómez, J. C., De León Aldaco, S. E., & Aguayo Alquicira, J. (2023). A review of hybrid renewable energy systems: Architectures, battery systems, and optimization techniques. *Eng*, *4*, 1446–1467. https://doi.org/10.3390/eng4020084

[15] Ferrucci, T., Fioriti, D., Poli, D., Barberis, S., Vannoni, A., Roncallo, F., …, & Gambino, V. (2023). Battery energy storage systems for ancillary services in renewable energy communities.In *E3S Web of Conferences, EDP Sciences*. https://doi.org/10.1051/e3sconf/202341403011

[16] Zhao, M., Zhang, J., Zhang, X., Duan, K., Dong, H., Lanceros-Méndez, S., …, & Zhang, Q. (2023). Application of high-strength, high-density, isotropic Si/C composites in commercial lithium-ion batteries. *Energy Storage Materials*, *61*, 102857. https://doi.org/10.1016/j.ensm.2023.102857

[17] Itani, K., & De Bernardinis, A. (2023). Review on new-generation batteries technologies: Trends and future directions. *Energies*, *16*, 7530. https://doi.org/10.3390/en16227530
[18] Bača, P., & Vanýsek, P. (2023). Issues concerning manufacture and recycling of lead. *Energies (Basel)*, *16*(11), 4468. https://doi.org/10.3390/en16114468
[19] Hernández-Callejo, L., Aguilar Jiménez, A., & Meza Benavides, C. (2023). Topic reprint advances in renewable energy and energy storage. https://doi.org/10.3390/books978-3-0365-9553-5, ISBN 978-3-0365-9553-5. Available at: https://www.mdpi.com/topics/EnergyStorage
[20] Kitaronka, S. (2022). Lead-acid battery. https://doi.org/10.6084/m9.figshare.19115057
[21] Carroquino, J., Escriche-Martínez, C., Valiño, L., & Dufo-López, R. (2021). Comparison of economic performance of lead-acid and li-ion batteries in standalone photovoltaic energy systems. *Applied Sciences (Switzerland)*, *11*(8), 3587. https://doi.org/10.3390/app11083587
[22] Bloom, I., Cole, B. W., Sohn, J. J., Jones, S. A., Polzin, E. G., Battaglia, V. S., . . . , & Case, H. L. (2001). An accelerated calendar and cycle life study of li-ion cells. *Journal of Power Sources*, *101*(2), 238–247. https://doi.org/10.1016/S0378-7753(01)00783-2
[23] Kim, S., Barnes, P., Zhang, H., Efaw, C., Wang, Y., Park, B., . . . , & Dufek, E. J. (2024). Calendar life of lithium metal batteries: Accelerated aging and failure analysis. *Energy Storage Materials*, *65*, 103147. https://doi.org/10.1016/j.ensm.2023.103147
[24] Babu, B. (2024). Self-discharge in rechargeable electrochemical energy storage devices. *Energy Storage Materials*, *67*, 103261. https://doi.org/10.1016/j.ensm.2024.103261
[25] Rahman, T., & Alharbi, T. (2024). Exploring lithium-ion battery degradation: A concise review of critical factors, impacts, data-driven degradation estimation techniques, and sustainable directions for energy storage systems. *Batteries*, *10*(7), 220. https://doi.org/10.3390/batteries10070220
[26] Xiao, W., Jia, J., Zhong, W., Liu, W., Wu, Z., Jiang, C., & Li, B. (2024). A novel differentiated control strategy for an energy storage system that minimizes battery aging cost based on multiple health features. *Batteries*, *10*(4), 143. https://doi.org/10.3390/batteries10040143
[27] Mosallanejad, B., & Akrami, M. (2024). Recent advances on electrolyte additives used in lead-acid batteries to enhance their electrochemical performances. *Journal of Energy Storage*, *97*, 112738. https://doi.org/10.1016/j.est.2024.112738
[28] Hioki (2020). Lead-acid battery handbook facilitating accurate measurement of lead-acid batteries. Available at: https://www.tekfinland.fi/wp-content/uploads/2021/09/HIOKI_Lead_acsid_Measurement_Guide_A_UG_BT0002E01.pdf
[29] Catherino, H. A., Feres, F. F., & Trinidad, F. (2004). Sulfation in lead–acid batteries. *Journal of Power Sources*, *129*(1), 113–120. https://doi.org/10.1016/j.jpowsour.2003.11.003
[30] Singh, A., Karandikar, P. B., & Kulkarni, N. R. (2021). Mitigation of sulfation in lead acid battery towards life time extension using ultra capacitor in hybrid electric vehicle. *Journal of Energy Storage*, *34*, 102219. https://doi.org/10.1016/j.est.2020.102219
[31] Gandhi, K. S. (2020). Modeling of sulfation in a flooded lead-acid battery and prediction of its cycle life. *Journal of the Electrochemical Society*, *167*(1), 013538. https://doi.org/10.1149/1945-7111/ab679b
[32] Bauknecht, S., Wätzold, F., Schlösser, A., & Kowal, J. (2023). Comparing the cold-cranking performance of lead-acid and lithium iron phosphate batteries at temperatures below 0 °C. *Batteries*, *9*(3), 176. https://doi.org/10.3390/batteries9030176
[33] Belgibayeva, A., Rakhmetova, A., Rakhatkyzy, M., Kairova, M., Mukushev, I., Issatayev, N., . . . , & Bakenov, Z. (2023). Lithium-ion batteries for low-temperature applications: Limiting factors and solutions. Journal of Power Sources, 557, 232550. https://doi.org/10.1016/j.jpowsour.2022.232550
[34] Prasad, U., Prakash, J., Kannan, A. N. M., Kamavaram, V., & Arumugam, G. K. (2023). Failure analysis of lead-acid batteries at extreme operating temperatures. *Battery Energy*, *2*(4), 20230008. https://doi.org/10.1002/bte2.20230008
[35] Guo, Q., Liu, S., Zhang, J., Huang, Z., & Han, D. (2024). Effects of charging rates on heat and gas generation in lithium-ion battery thermal runaway triggered by high temperature coupled with overcharge. *Journal of Power Sources*, *600*, 234237. https://doi.org/10.1016/j.jpowsour.2024.234237
[36] Crockford, H. D. (1937). *Gassing characteristics of flat plate lead-acid storage cells during discharge*. USA: Navy Department, Bureau of Engineering. https://apps.dtic.mil/sti/trecms/pdf/AD1155465.pdf
[37] Gabler, H., Sauer, D. U., & Jossen, A. (1995). *A systematic effort to define evaluation and performance parameters and criteria for lead-acid batteries in PV systems*. [Online]. Retrieved from: https://www.researchgate.net/publication/287336077
[38] Gräf, D., Marschewski, J., Ibing, L., Huckebrink, D., Fiebrandt, M., Hanau, G., & Bertsch, V. (2022). What drives capacity degradation in utility-scale battery energy storage systems? The impact of operating strategy and temperature in different grid applications. *Journal of Energy Storage*, *47*, 103533. https://doi.org/10.1016/j.est.2021.103533
[39] Faanzir, F. (2021). Determining the shortest charging time of batteries using SOC set point at constant current – constant voltage mode. *Przegląd Elektrotechniczny*, *1*(4), 56–61. https://doi.org/10.15199/48.2021.04.09
[40] Liu, C. L., Chiu, Y. S., Liu, Y. H., Ho, Y. H., & Huang, S. S. (2013). Optimization of a fuzzy-logic-control-based five-stage battery charger using a fuzzy-based taguchi method. *Energies (Basel)*, *6*(7), 3528–3547. https://doi.org/10.3390/en6073528
[41] Huang, S.-J., Huang, B.-G., & Pai, F.-S. (2013). Fast charge strategy based on the characterization and evaluation of LiFePO4 batteries. *IEEE Transactions on Power Electronics*, *28*, 1555–1562. https://doi.org/10.1109/TPEL.2012.2209184
[42] Banguero, E., Correcher, A., Pérez-Navarro, Á., Morant, F., & Aristizabal, A. (2018). A review on battery charging and discharging control strategies: Application to renewable energy systems. *Energies*, *11*, 1021. https://doi.org/10.3390/en11041021
[43] Escobar, E. D., Betancur, D., & Isaac, I. A. (2024). Optimal power and battery storage dispatch architecture for microgrids: Implementation in a campus microgrid. *Smart Grids and Sustainable Energy*, *9*(2), 27. https://doi.org/10.1007/s40866-024-00210-8
[44] Rina, Z. S., Amin, N. A. M., Hashim, M. S. M., Majid, M. S. A., Rojan, M. A., & Zaman, I. (2017). Development of a microcontroller-based battery charge controller for an off-grid photovoltaic system. In *IOP Conference Series: Materials Science and Engineering*. https://doi.org/10.1088/1757-899X/226/1/012138

[45] Díaz, P., & Egido, M. Á. (2003). Experimental analysis of battery charge regulation in photovoltaic systems. *Progress in Photovoltaics: Research and Applications*, *11*(7), 481–493. https://doi.org/10.1002/pip.509

[46] Wang, K., Wu, D., Chang, C., Zhang, J., Ouyang, D., & Qian, X. (2024). Charging rate effect on overcharge-induced thermal runaway characteristics and gas venting behaviors for commercial lithium iron phosphate batteries. *Journal of Cleaner Production*, *434*, 139992. https://doi.org/10.1016/j.jclepro.2023.139992

[47] Qian, L., Yi, Y., Zhang, W., Fu, C., Xia, C., & Ma, T. (2023). Revealing the impact of high current overcharge/overdischarge on the thermal safety of degraded li-ion batteries. International Journal of Energy Research, 2023, 2023. https://doi.org/10.1155/2023/8571535

How to Cite: Karaman, C. (2024). Aging Retardation of Lead-Acid Batteries by Adjusting Charge Controller Threshold Values in Off-grid Photovoltaic System. *Archives of Advanced Engineering Science*. https://doi.org/10.47852/bonviewAAES42024076